Technical Physics, Vol. 48, No. 6, 2003, pp. 749–756. Translated from Zhurnal Tekhnicheskoĭ Fiziki, Vol. 73, No. 6, 2003, pp. 90–98.

**OPTICS,
QUANTUM ELECTRONICS**

Photochromic Reactions in Silver Nanocomposites with a Fractal Structure and Their Comparative Characteristics

S. V. Karpov*, A. K. Popov*, and V. V. Slabko**

** Kirenskiĭ Institute of Physics, Siberian Division, Russian Academy of Sciences, Akademgorodok, Krasnoyarsk, 660036 Russia*

e-mail: karpov@iph.krasn.ru

*** Krasnoyarsk State Technical University, Krasnoyarsk, 660074 Russia*

Received October 2, 2002

Abstract—Conditions for a change in the polarization selectivity of dips in the plasmon absorption spectra of fractal silver nanocomposites irradiated by pulsed laser radiation are studied. The energy thresholds of the polarization selectivity are evaluated, and the polarization and spectral threshold characteristics are compared. Mechanisms behind the correlation between the fractal structure of the nanocomposites, on the one hand, and their optical and photochromic properties, on the other hand, are discussed. *© 2003 MAIK "Nauka/Interperiodica".*

INTRODUCTION

Photochromic processes in silver nanocomposites containing fractal clusters, or fractal aggregates (FAs), were discovered and characterized for the first time in [1]. These processes in fractal media are of interest for many reasons. First, they may be related to the unique nonlinear optical properties of FAs [2]. The giant (10^6 times) enhancement of degenerate four-photon parametric scattering (DFPS) upon silver particle aggregation, the effect observed as early as in pioneering experiments [3, 4], gives special significance to the study of such media, including the need to estimate the role of attendant photochromic processes. Second, such media appear to be promising for polychromic data recording [5].

The effect discovered in [1] was as follows. The pulsed laser irradiation of colloidal silver aggregates embedded in gelatin matrices (the volumetric aggregate concentration was on the order of 10^{-5}) "burned out" a relatively narrow (80–100 nm) long-lived dip near the irradiation wavelength in the spectrum of absorption of light with the same linear polarization as that of the irradiating laser pulse. Furthermore, the width of the dip was close to the plasmon absorption bandwidth for an individual particle.

In transmitted light, one can see a spot near the irradiation area that has the same color as incident radiation. This phenomenon is associated with the so-called photomodification of FAs (the photoinduced modification of their structure), which occurs in the case of the local (spatially selective) absorption of radiation with a given frequency and polarization by resonant particles of FAs.

This phenomenon has been clearly explained by invoking the theory of optical properties of fractal clusters (the OPFC theory) [6–8], which establishes a one-to-one correspondence between the structural and optical properties of FAs.

The aim of this work is (i) the determination of energy thresholds for the polarization selectivity of photoinduced dips in the absorption spectra taken from association silver colloids and (ii) the interpretation of related data in terms of the fractal structure of the aggregates, which is responsible for a number of unique properties of these objects.

OPTICAL PROPERTIES OF FRACTAL SILVER NANOCOMPOSITES

The optical properties of silver nanoparticles are specified by surface plasmon resonance with a near-Lorentzian profile of the absorption band with a uniform width of about 80 nm and a peak at $\lambda \simeq 420$ nm in hydrosols.

It is known that, during the evolution of a sol, the majority of isolated particles aggregate to form fractal structures (see references in [6]). Such structures are observed, in particular, when clusters are deposited on a substrate during the laser evaporation of a metallic target [9].

When combined into FAs, the particles cannot be considered as isolated; therefore, the interaction of radiation-induced oscillating dipole moments should be taken into account. Let us consider the effect of such interaction on the absorption spectra in greater detail.

Works [6, 7, 9, 10] have evidenced the strong influence of nearby particles on the spectrum of any particle incorporated into an FA. This causes a substantial shift in the frequency ω_r of natural optical resonances of the particles. The reason for the shift is electrodynamic par-

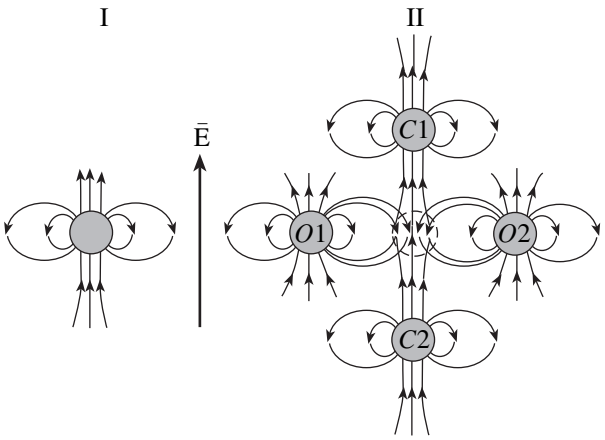

Fig. 1. Formation of the self-consistent field around an *i*th particle (marked by the dashed circle at the center) upon the dipole–dipole interaction of the particle in a varying electric field **E** (for the symmetric environment of the *i*th particle). I, configuration of the lines of electric force of the self-induced dipole at the *i*th particle; II, configuration of the lines of electric force of the dipoles induced by pairs of particles that are collinear with (*C*1, *C*2) and orthogonal to (*O*1, *O*2) the field at the site of the *i*th particle.

ticle interaction (with the prevailing effect of the nearest particle). It was shown (e.g., in [6]) that the effect of nearby particles shows up as a split of the intrinsic resonance (with a frequency ω_r) of a single initially isolated particle into two, lower frequency (ω_l) and higher frequency (ω_h), peaks. It is noteworthy that the shift of the lower frequency resonance is nearly twice as large as that of the higher frequency one [6, 10]. Because of this, the plasmon absorption spectrum of FAs broadens significantly but asymmetrically, covering the entire visible range and a part of the IR range (see, e.g., [10]).

Due to the interaction of a particle with its nearest neighbor, the resonance frequency shifts by a value of $\Delta\omega \approx \Omega_f$, where Ω_f is the characteristic (mean) value of the frequency shift. This parameter defines the characteristic scale of the broadening and of the low-frequency shift (and, accordingly, the extension of the long-wave wing) of the FA spectrum relative to the spectrum of an isolated particle [8]:

$$\Omega_f = \omega_m(R_n/R_0)^3, \quad (1)$$

where R_0, R_n, and ω_m are, respectively, the characteristic spacing between neighboring particles in an FA, particle size, and resonance frequency of the particles. In other words, the frequency shift is inversely proportional to the particle spacing cubed. In the presence of an adsorption layer around the particles, this spacing may exceed R_n only slightly; hence, $\Omega_f \simeq \omega_m$. That is to say, the effect of electrodynamic interaction between nearby particles in a fractal is so high that their resonances at frequencies comparable to the natural resonance frequency shift. An increase in the particle spacing, e.g., by thickening the adsorption layer or increasing the particle size, would decrease the resonance shifts and, accordingly, shrink the long-wave wing of the fractal spectrum.

If the frequency of external radiation falls into the fractal's absorption band, there will always be found resonant particles (or, more specifically, pairs of resonant particles) that are far apart within an FA. The fraction of such particles is $\Gamma/\Omega_f \ll 1$, where Γ is the plasmon absorption bandwidth. Therefore, different parts of the fractal will absorb monochromatic radiation independently because of the heavily asymmetric broadening (due to the dispersion of pair interactions) of the absorption spectrum of the fractal.

In hydrosols, the long-wave wing of the spectrum expands when FAs form. This is because of the great diversity of possible environments near a particular particle involved in an FA. In this case, the relative fraction of closely spaced pairs of particles grows. In addition, as the FA circumference elongates, the local anisotropy of the environment around the particles is enhanced. The appearance of the short-wave branch of the FA spectrum, which is twice as short as the long-wave one (on the frequency scale), is associated with a high-frequency peak of interacting pairs that appears in the absorption spectrum.

Electrodynamic interactions in a set of closely spaced metal particles are a ready illustration of how the fractal geometry and local anisotropy of association colloids influence their optical properties. Qualitatively, this effect is described in Fig. 1.

Consider the isotropic case. A feature of dipole–dipole interaction is that the self-consistent field produced near an *i*th particle by all other fractal particles vanishes when averaged over the spherically symmetric particle distribution. From Fig. 1 it follows that lines of electric force of the dipoles induced on particles that are oriented orthogonally to and collinearly with the applied electric field enter the *i*th particle in opposite directions and almost completely cancel each other (provided that the contribution from all its neighbors is strictly averaged). Obviously, a net addition to the local field induced by all the particles evenly distributed around the *i*th particle tends to zero as the environment of the *i*th particle becomes progressively more isotropic. Note that such a statement holds only in the 3D case, when averaging must take into account not only collinear pairs oriented along the *Z* axis but also orthogonal pairs oriented along the *X* and *Y* axes (the number of the latter pairs turn out to be twice that of collinear pairs). The need for considering collinear pairs is dictated by the fact that, in dipole–dipole interaction, the interaction energy of collinear pairs is twice as high as that of orthogonal ones [11].

The situation changes drastically when the particles are integrated into FAs, i.e., when most particles around a given one are surrounded by either orthogonally oriented or collinear pairs (in terms of their projections to the field direction). In other words, the environment of

an ith particle is severely anisotropic under these conditions. Note that colloidal FAs typically produce branched chain structures. Certainly, one may find a number of less anisotropic local configurations of the particles. In Fig. 1, they would appear if one of the particles in collinear or orthogonal pairs were absent, i.e., if the self-consistent field were generated by three (or five in the 3D case) surrounding particles.

Let us consider the effect of local anisotropy for the highest anisotropy case when only orthogonal ($O1$, $O2$) or only collinear ($C1$, $C2$) pairs are left in Fig. 1. In terms of this simplified model, the addition to the local field around an ith particle is negative if the orthogonal pairs are left. It will also be recalled that, for this configuration, the frequency of the applied field falls into the short-wave part of the fractal spectrum.

For a constant initial strength of the applied field and the same damping constants, this is equivalent to a decrease in the polarizability χ of the ith particle in an aggregate under the effect of the orthogonal pairs. In turn, a decrease in the polarizability is equivalent to an increase in the detuning $\Omega = |\omega_r - \omega|$ ($\chi \sim \Omega^{-1}$) because of the shift of ω_r toward higher frequencies. That is the reason why the high-frequency branch of the FA absorption spectrum somewhat broadens.

Using a similar line of reasoning for the collinear ($C1$, $C2$) pairs and taking into account that the addition to the local field near the ith particle is now positive, we arrive at the conclusion that this situation is equivalent to the case when the polarizability of the particle grows. Here, an increase in the polarizability of the ith particle within a fractal due to dipole–dipole interaction corresponds to a decrease in the detuning $\Omega = |\omega_r - \omega|$ because of the shift of the resonance frequency ω_r toward lower frequencies. This explains the appearance of the long-wave wing in the FA absorption spectrum.

Quantitatively, corrections to the local fields and to the positions of resonant absorption bands were considered in detail by Aver'yanov [12–14]. His model has been used to advantage in liquid-crystal optics.

Let us analyze several expressions that shed light upon the problem solved in [12–14]. To a linear approximation, with the Lorentz tensor L introduced in the expression $\mathbf{P} = N\chi_0 f\mathbf{E}$, a shift of the absorption band maximum in response to a change in the local field is given by formula (2). In the above expression, $\mathbf{P}$ is the polarization of a medium that is related to a macroscopic field $\mathbf{E}$ (including a correction for depolarization), $f = 1 + L(\varepsilon - 1)$ is the local-field tensor, χ_0 is the tensor of the dipole polarizability of particles, and N is the particle concentration in the medium. Then [12],

$$\omega_r' = \omega_r - \frac{\omega_p^2 F_{12} L_j (f_j)_b}{2\omega_r}\left(1 - \frac{(f_j)_b}{6L_j(\varepsilon_j)_b}\right). \qquad (2)$$

Here, ω_r is the initial resonance position with regard for the environmental influence, ω_r' is the resonance position after the local field has changed, ω_p is the plasma frequency, F_{12} is the transition oscillator strength (in our case, it corresponds to the excitation of a particle's surface plasmon), L_j are the diagonal components of the Lorentz tensor, $j = \{xx, yy, zz\}$ (in general, $L_j = 1/3 - B_j/4\pi N$), B_j is the sum over dipoles within the Lorentz sphere (in particular, $B_{xx} = \Sigma(1/r_i^3 - 3X_i^2/r_i^5)$, where $\mathbf{r}_i$ is the radius vector of an ith particle in the Lorentz sphere with the origin placed at the center of the sphere and X_i is the coordinate of the vector), $(f_j)_b = 1 + L_j[(\varepsilon_j)_b - 1]$ are the diagonal components of the local-field tensor that take into account an increase in the effective local field strength with respect to the strength of the macroscopic field of a light wave in the medium ($\mathbf{E}_{\text{eff}}^{\text{loc}} = f\mathbf{E}$), $(\varepsilon_j)_b = (\varepsilon)_b\delta_{ij}$ is the background permittivity imposed by all resonances in the medium except for that under consideration, and δ_{ij} is the Kronecker symbol. The product $L_j(f_j)_b$ is responsible for the configuration and interaction of the particles in the system.

For the isotropic arrangement of the particles, the equilibrium value of the diagonal components is $L_j = 1/3$. For pairs of particles that are collinear with the field (when the field is directed along the Z axis), the maximal value of L_j in expression (2) tends to unity (the components L_j and ε_j with $j = \{zz\}$ are used). For orthogonal pairs, L_j tends to zero (L_j and ε_j with $j = \{xx, yy\}$ are used).

With such values of L_j, the parenthesis in (2), which specifies the sign of the resonance frequency shift $(\omega_r' - \omega_r)$, can be either positive or negative depending on the particle configuration. Note that expression (2) is accurate if the inequality $F_{12}/3 \le \omega_r\Gamma(\varepsilon_j)_b/\omega_p^2(f_j)_b^2$ holds (medium- and low-absorption bands). However, it is helpful in qualitatively treating the effect.

For strong-absorption bands, we have expression

$$\omega_r' = \omega_r - \frac{\omega_p^2 F_{12} L_j (f_j)_b}{2\omega_r} + \Gamma/2\sqrt{3}, \qquad (3)$$

which yields the same law for frequency shift sign under similar conditions.

Thus, since the environments of most of the particles in an FA are locally anisotropic, additions to the local field do not cancel each other (Fig. 1). For this reason, the effect of significant enhancement of local electromagnetic fields [15] is inherent mostly in fractal structures. To check this assumption, the absorption spectra of Ag sols with a stochastically uniform particle distribution were calculated in terms of the OPFC theory [7]. For this case, the broadening of the absorption bands appeared to be the same as for media with ordered particle distributions or for media with isolated particles.

Note also that the FA spectra will be broader for metal particles, which have larger matrix elements of transition electric dipole moments that characterize

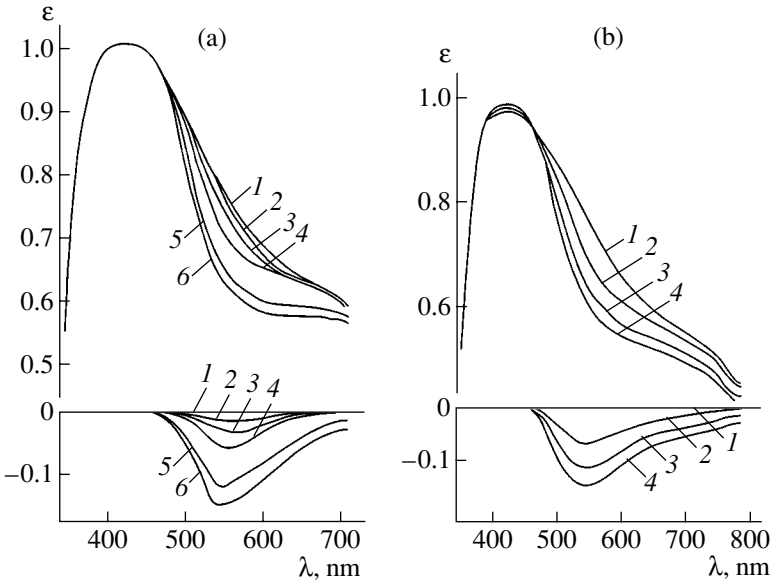

Fig. 2. Absorption spectrum (at the top) and differential spectrum (at the bottom) of irradiated and (*1*) nonirradiated silver aggregates subjected to picosecond and nanosecond pulses with λ = 540 nm. (a) The number of pulses with W = 2 mJ/cm^2 and τ = 30 ps is (*2*) 1, (*3*) 10, (*4*) 20, (*5*) 80, and (*6*) 230. (b) Single-pulse irradiation with W = (*2*) 8, (*3*) 10, and (*4*) 12.4 mJ/cm^2; τ = 15 ns.

optical resonance. For particles that have optical polarizabilities lower than those of metal particles, dipole–dipole interaction causes a smaller shift of resonances.

Analytical expressions that relate quantitatively the fractal dimension of aggregates to the broadening of their absorption spectra can be derived only in the binary approximation to the OPFC theory (in view of the well-known limitations involved in this approximation) [8].

A description of the FA absorption spectra that is based on the rigorous OPFC model is given elsewhere [6, 7, 10]. In this case, however, an analytical relationship between the broadening and fractal dimension is impossible to find, because (i) the model is additive and (ii) the number of equations for FA polarizability by which the properties of the model are described exceeds N_0^3 (N_0 is the number of particles). Yet, a correlation between the absorption spectrum and the fractal dimension persists, since fractal geometry is featured by aggregates over which the summation is carried out.

EXPERIMENTAL RESULTS AND DISCUSSION

FA photomodification is most pronounced in media with a near-limiting degree of association. Association silver sol consists of aggregates 0.1–1.0 μm or more in size. Aggregates, in turn, integrate particles of radius 5–10 nm. Comparing the number of particles and the sizes of aggregates in micrographs yields the fractal dimension $D \simeq 1.7$, which is typical of such objects.

The plasmon absorption spectrum of a hydrosol with unassociated Ag particles has a sharp peak at $\lambda_{pl} \simeq$ 420 nm and Γ = 80–100 nm. Of association media, a broad absorption band in the visible and near-IR (λ = 1.0–1.5 μm) ranges is characteristic (see, e.g., [10]).

Aggregated Ag sols (or Ag aggregates in gelatin) were irradiated by second-harmonic pulses from $Y_3Al_5O_{12}$: Nd and $YAlO_3$: Nd lasers (λ = 532 and 540 nm, respectively) and also by radiation generated by stimulated Raman scattering in acetone (λ = 641 nm). Giant (τ ≃ 10 ns) and ultrashort (τ ≃ 30 ps) pulses were applied.

Figures 2 and 3 show irradiation-induced changes in the absorption spectra of the sols, i.e., dips near the lasing wavelengths. It is seen that the depth and width of the gaps grow with both the number and energy of irradiation pulses. This is because the burning out of the dips is a process of a threshold nature (or highly nonuniform in energy). In the hydrosol (Figs. 2a, 2b) at τ = 15 ns, the spectral dip near λ = 532 nm is observed at a pulse energy density W = 4–10 mJ/cm^2. For picosecond pulses, the threshold energy can be several times lower than for nanosecond radiation.

The characteristic width of the dips (about 3500 cm^{-1}) is close to the symmetric width of the absorption band for individual particles in an unassociated hydrosol (3500–5000 cm^{-1}) and is much smaller than the width of the FA absorption band (more than 20 000 cm^{-1}). The narrowest dips (1800 cm^{-1}) were observed in the spectra of aggregates recorded in holographic emulsion [1]. It should be noted that an asymmetric broadening (within Δλ = 15 nm) of the absorption band is observed even in the unassociated hydrosol due to its polydisper-

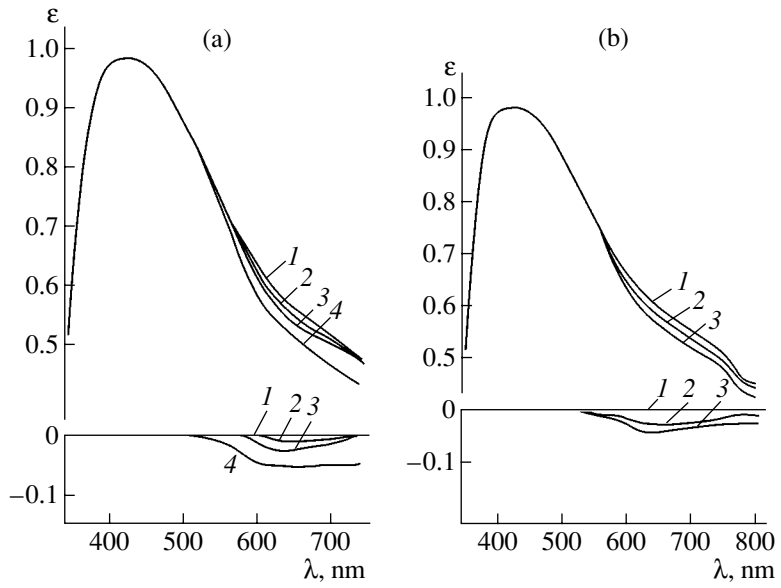

Fig. 3. The same as in Fig. 2 for λ = 641 nm. (a) (*2*) 20 pulses with $W = 2$ mJ/cm^2, (*3*) 120 pulses with $W = 2$ mJ/cm^2, and (*4*) one 8-mJ/cm^2 pulse; τ = 30 ps. (b) (*2*) 20 and (*3*) 40 pulses with $W = 4$ mJ/cm^2; τ = 15 ns.

sity and a spread in the resonance frequency for particles from 5 to 30 nm in size. Also, even microaggregates present in the sol cause an additional broadening of the plasmon absorption band.

According to today's concepts, dips related to photomodification are explained by burning out particles for which the shift of the resonance frequency (because of dipole–dipole interaction) equals the incident radiation frequency. It is this burning out (breakage) that is responsible for the threshold character of the photomodification process.

Estimates show that each resonant particle of a fractal for $W = 1.5$ mJ/cm^2 and a particle concentration of 10^{12} cm^{-3} absorbs about 3×10^5 photons per pulse. This value equals or somewhat exceeds the energy needed to sublimate a particle with a radius of 10 nm. With τ = 30 ps, the area of absorbed energy localization, $d \propto \sqrt{\tau}$, is on the order of the particle size; with τ = 15 ns, this area covers several particles. This is the reason for the high value of the threshold energy and the partial loss in frequency and polarization selectivity in the case of long pulses, which is observed in experiments.

Among the specific features of photomodification, of interest is the fact that, roughly within an hour after the irradiation of the entire cuvette with the hydrosol, a spectral dip may broaden and shift slightly toward longer waves. In this case, the peak due to plasmon absorption somewhat grows. This finding may be related to photostimulated aggregation [16–19] when microaggregates or a small fraction of free particles are present in the medium.

Stable (at least for a month) dips in the absorption spectrum were observed for silver aggregates in gelatin (Figs. 2, 3). Still more stable dips were found upon using polyacrylamide matrices in our experiments. For example, a number of the samples irradiated have retained spectral selectivity since 1987. Such a slow relaxation can be attributed to the fact that here particles have a lower mobility than in the liquid.

Note that the threshold energy of photomodification may somewhat increase if sol particles are surrounded by a polymeric adsorption layer.

Along with the dip near the laser wavelength in the FA absorption spectrum, there appears polarization selectivity in the irradiation zone, which depends on the incident radiation polarization. This effect is explained by the fact that resonance in the collinear configurations of pairs, shifts, as was already noted, toward lower frequencies relative to the resonance frequency of an isolated particle ($\omega_r' < \omega_r$). For orthogonal pairs, a shift toward higher frequencies ($\omega_r' > \omega_r$) is observed. Hence, an important conclusion follows: when interacting with the aggregate, linearly polarized monochromatic radiation must impart nearby particles a certain arrangement. It will be recalled that a radiation with a wavelength from the long-wave wing interacts only with collinear pairs.

Figure 4 demonstrates the variation of the dip near the laser wavelength λ = 540 nm (τ = 15 ns) in the differential absorption spectrum of aggregated silver (embedded in the gelatin matrix). Bearing in mind that polarization selectivity arises when the radiation interacts with collinear or orthogonal pairs of particles, one can infer that, in an FA, the radiation interacts with both simultaneously. Accordingly, a radiation with a wavelength from only the long-wave or short-wave branch of

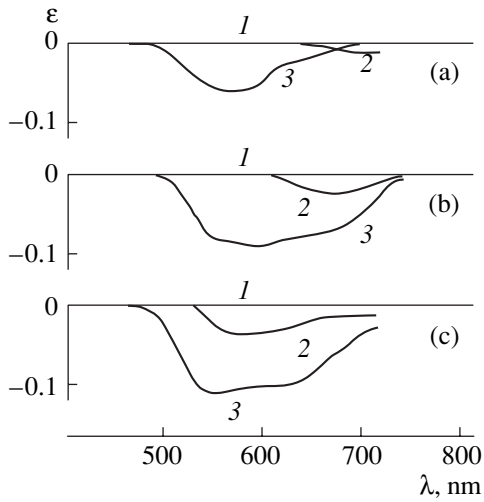

Fig. 4. Variation of the polarization of the spectral dip (in the differential absorption spectra) upon irradiating by pulses with $\lambda = 540$ nm and $\tau = 15$ ns. W = (a) 7, (b) 30, and (c) 60 mJ/cm^2. (*1*) Nonirradiated medium, (*2*) irradiated medium with linear polarization orthogonal to incident light, and (*3*) polarization corresponding to that of incident light.

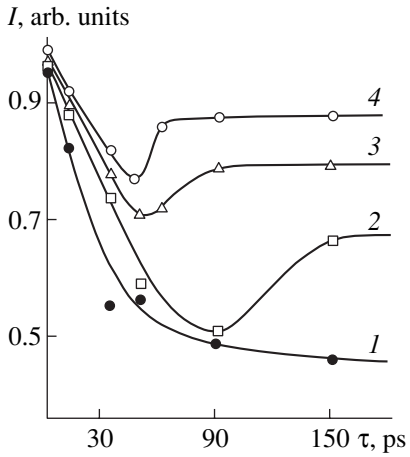

Fig. 5. Amplitude of the optical response to DFPS in the aggregated silver hydrosol vs. elapsed time from the application of the pulses ($\lambda = 540$ nm, $\tau = 30$ ps). W = (*1*) 8.25, (*2*) 20.76, (*3*) 24.75, and (*4*) 30 mJ/cm^2.

the absorption spectrum causes two dips to appear simultaneously: one at $\lambda > \lambda_{pl}$ and the other at $\lambda < \lambda_{pl}$ with their polarizations being mutually orthogonal.

As follows from Fig. 4, the increase in the pulse energy density from 7 to 60 mJ/cm^2 leads to a broadening of the low-frequency dip primarily to the long-wave wing. This is related to the fact that nonresonant pairs of particles start being involved in the process with the resulting degradation of the spectral selectivity. Also, the dip in the orthogonal polarization becomes deeper possibly because of the pulsed-induced break of local anisotropy near resonant particles.

The aforesaid is in complete agreement with current concepts [20] of processes disturbing the locality of interactions above the energy threshold.

To observe the polarization effect upon burning out the spectral dip, the FAs irradiated should be spatially fixed with the use of nondestructive matrices. The relaxation times of photochromic processes far exceed the lifetime of the polarization effect. For example, the visually estimated time of tint diffusion blurring in the irradiation zone of hydrosols is not more than a few seconds. As for polarization selectivity, its lifetime τ_l in the irradiation zone is several microseconds or less, depending on the rotational diffusion of the aggregates upon Brownian motion. As is known, the angle of rotation Θ_0 of a Brownian particle and the time of rotation are related by the expression

$$\sin^2\Theta_0 = 2/3[1 - \exp(-6D_{rot}t)],$$

where $D_{rot} = kT/8\pi\eta(2R_a)^3$ is the rotational diffusion coefficient, k is the Boltzmann constant, T is the ambient temperature, $2R_a$ is the dimension of an aggregate, and η is the dynamic viscosity.

With $\eta = 0.001$ Pa s [16], $a = 10^{-7}$ m, and $\Theta_0 = 45°$, the rotational diffusion time corresponding to this angle is on the order of 10^{-4}–10^{-3} s. From this value, the lifetime τ_l can be found.

To estimate the evolution time of the photomodification process, we experimentally studied the kinetics of degenerate four-photon parametric interaction (under conditions of phase conjugation) with FAs in Ag hydrosols at different energy densities of picosecond second-harmonic ($\lambda = 540$ nm) pulses from a $YAlO_3$: Nd laser [21], including those exceeding the energy threshold of photomodification.

A diffraction grating in the medium under study was formed by applying 30-ps pulses, with the probe pulse being applied with a controllable delay. Figure 5 shows the amplitude of the optical response to DFPS in the associated Ag hydrosol versus elapsed time from irradiating pulses ($\tau = 30$ ps) for different energy densities of the pulses. The inertial part of the amplitude is related to the variation of the sol absorption coefficient due to the photomodification of silver aggregates in the sol irradiated.

It was found that, when the pulse energy density exceeds the threshold, along with the fast response (observed at $t \le 50$ ps), the slow response, which correlates with the onset of FA photomodification [4], appears (at $t > 50$ ps). The time of its appearance depends on the pulse energy density and varies from 150 to 50 ps as the total energy density of pumping pulses (without considering Fresnel losses) increases from $W = 20.76$ to 24.75 and then to 30 mJ/cm^2. With $W = 8.25$ mJ/cm^2 or less, the inertial response was absent (Fig. 5). To be precise, we note that the energy of a laser pulse was distributed among two reference pulses, which formed the refractive index grating, and one probe pulse in roughly equal proportions.

The kinetics of the photomodification process, which starts when the absorbed energy per pulse is sufficient to sublimate a particle of radius 10 nm, is defined by the following expansion of sublimation products or by the modification of the FA structure until the depth of optical modulation (relative to the equilibrium value) due to these processes becomes below the sensitivity limit of a measuring method used.

Another view of the photomodification process (and, hence, its kinetics) should also be taken into consideration. In [22], the possibility of photoinduced modifications in the FA structure that arise in the light wave field under the action of resulting dipole–dipole interactions was analyzed. The authors of [22] believe that this process may both induce dichroism and favor the coalescence of resonant particles heated up (even if insignificantly) by the radiation absorbed.

The threshold (in energy) character of photomodification was analyzed in [20, 23, 24], where the presence of two thresholds was reported. The first one is related to the dip burned out on the short-wave side of the FA absorption peak. Physically, this threshold is due to a change in the polycrystalline structure of individual particles. The second threshold is associated with two dips appearing simultaneously. One arises in the long-wave wing near the frequency of a modifying radiation; the other, in the short-wave branch. In this case, as was noted above, the frequency of the low-frequency dip differs from the maximal absorption frequency of the unassociated hydrosol by a value that is twice as large as the shift of the high-frequency dip. Measurements [20, 23] showed that the low-frequency dip is deeper and its polarization is orthogonal to that of the high-frequency dip, which is fully consistent with the existing theoretical concepts.

In the case of short pulses, the energy threshold of photomodification depends largely not on the pulse intensity but on the energy density or, eventually, on the number of photons absorbed by a resonant particle. However, the radiation intensity, which specifies the strength of the optical wave field, should also be taken into account, since this parameter is responsible for optical damage to the crystal lattice of a particle during energy exchange with free electrons generated by the electromagnetic wave. In the case of long pulses (in particular, free-running pulses with $\tau = 0.1$ ms and $W = 0.1$ J/cm^2) or continuous radiation, photomodification ceases [1]. An increase in the pulse duration is also accompanied by more intense heat exchange.

The duration of irradiating pulses also has an effect on the spectral characteristics of photomodification. In going from nanosecond to picosecond pulses, the area of absorbed energy localization shrinks and the spectral dips become narrower. With nanosecond pulses, the collapse (reconstruction) of resonant domains in FAs also covers nearby particles whose resonance frequencies may differ from those of the resonant domains. This, in particular, explains why the spectral width of the dips somewhat increases, as demonstrated in Figs. 2 and 3.

One more feature of photomodification is that the dip becomes wider as the wavelength approaches that of absorption maximum (410–420 nm) [5, 20, 23, 24]. This is because the closer the wavelength to the initial plasmon maximum, the greater the number of resonant particles. On the contrary, the number of closely spaced pairs of particles with a large shift of resonances decreases away from the plasmon absorption maximum. This feature is substantiated by the fact that the threshold energy drops with distance to this maximum, since the radiation is absorbed by a lesser number of resonant particles. This is one more confirmation that the energy absorbed is distributed over the whole aggregate but localizes in resonant domains in the first case and in domains fairly distant from each other in the second case. Since, as was mentioned above, the collapse of resonant domains may partially cover adjacent FA areas, such a delocalization may involve a great amount of nonresonant particles in the process.

In [5, 23], structural changes in FAs induced by pulsed laser irradiation were examined. It appeared that FAs irradiated contain large spherical and ellipsoidal forms instead of initial particles. The fraction of the new forms depended on the incident radiation wavelength. For $\lambda = 450$, 540, and 1079 nm, this fraction equaled 0.7, 0.3, and 0.1, respectively.

The results of numerical simulation of photomodification in terms of the OPFC theory were reported in [20, 23, 24]. It was shown that a dip similar to that observed in our experiments appears in the FA absorption spectrum after the removal of resonant particles from FAs.

In spite of major achievements in studying the photomodification of noble-metal-based FAs, a physical model of this phenomenon has not yet been elaborated and a mechanism that can explain the entire body of experimental data and include the effect of attendant processes is still lacking. Research in this field continues.

CONCLUSIONS

(1) Photomodification of colloid fractals aggregates of metallic sols experimentally confirms the fact that the plasmon absorption band in their spectra broadens asymmetrically, since the width of the dip burned out is close to that of the symmetric absorption band for isolated particles.

(2) The polarization effect also unambiguously indicates the asymmetric broadening of the FA spectrum and, hence, the locality of photomodification. Furthermore, this effect follows from the local anisotropy of the fractals and also from the interaction of radiation with pairs of particles configured collinearly with and orthogonally to the field.

(3) The transition from nanosecond to picosecond irradiation pulses makes it possible to narrow the area of absorbed energy localization and, accordingly, produce narrower spectral dips.

(4) The energy threshold of photomodification largely depends not on the pulse intensity but on the energy density or, eventually, on the number of photons absorbed by each resonant particle in an FA. The energy threshold drops with increasing pulse wavelength.

REFERENCES

1. S. V. Karpov, A. K. Popov, S. G. Rautian, *et al.*, Pis'ma Zh. Éksp. Teor. Fiz. **48**, 528 (1988) [JETP Lett. **48**, 571 (1988)].
2. Yu. E. Danilova, N. N. Lepeshkin, S. G. Rautian, *et al.*, Physica A **241**, 231 (1997).
3. S. G. Rautian, V. P. Safonov, P. A. Chubakov, *et al.*, Pis'ma Zh. Éksp. Teor. Fiz. **47**, 200 (1988) [JETP Lett. **47**, 243 (1988)].
4. A. V. Butenko, Yu. E. Danilova, P. A. Chubakov, *et al.*, Z. Phys. **17**, 283 (1990).
5. V. P. Safonov, V. M. Shalaev, V. M. Markel, *et al.*, Phys. Rev. Lett. **80**, 1102 (1998).
6. V. A. Markel', L. S. Muratov, and M. I. Shtokman, Zh. Éksp. Teor. Fiz. **98**, 819 (1990) [Sov. Phys. JETP **71**, 455 (1990)].
7. V. M. Markel, V. M. Shalaev, E. V. Stechel, *et al.*, Phys. Rev. B **53**, 2425 (1996).
8. V. M. Shalaev and M. I. Shtokman, Zh. Éksp. Teor. Fiz. **92**, 509 (1987) [Sov. Phys. JETP **65**, 287 (1987)].
9. A. I. Plekhanov, G. L. Plotnikov, and V. P. Safonov, Opt. Spektrosk. **71**, 775 (1991) [Opt. Spectrosc. **71**, 451 (1991)].
10. S. V. Karpov, A. L. Bas'ko, A. K. Popov, *et al.*, Kolloidn. Zh. **62**, 773 (2000).
11. L. D. Landau and E. M. Lifshitz, *Course of Theoretical Physics*, Vol. 2: *The Classical Theory of Fields* (Nauka, Moscow, 1973; Pergamon, Oxford, 1975).
12. E. M. Aver'yanov, *Local Field Effects in Liquid Crystal Optics* (Nauka, Novosibirsk, 1999).
13. E. M. Aver'yanov, Pis'ma Zh. Éksp. Teor. Fiz. **66**, 805 (1997) [JETP Lett. **66**, 847 (1997)].
14. E. M. Aver'yanov, Opt. Zh. **65** (7), 5 (1998).
15. V. M. Shalaev, E. Y. Poliakov, and V. A. Markel, Phys. Rev. B **53**, 2437 (1996).
16. *Tables of Physical Quantities*, Ed. by I. K. Kikoin (Nauka, Moscow, 1970).
17. S. V. Karpov, A. L. Bas'ko, S. V. Koshelev, *et al.*, Kolloidn. Zh. **59**, 765 (1997).
18. S. V. Karpov, A. K. Popov, and V. V. Slabko, Pis'ma Zh. Éksp. Teor. Fiz. **66**, 97 (1997) [JETP Lett. **66**, 106 (1997)].
19. S. V. Karpov, V. V. Slabko, and G. A. Chiganova, Kolloidn. Zh. **64**, 474 (2002).
20. Yu. E. Danilova, S. G. Rautian, and V. P. Safonov, Izv. Ross. Akad. Nauk, Ser. Fiz. **60** (3), 56 (1996).
21. S. V. Karpov, A. K. Popov, and V. V. Slabko, Izv. Ross. Akad. Nauk, Ser. Fiz. **60** (6), 43 (1996).
22. V. P. Drachev, S. V. Perminov, S. G. Rautian, *et al.*, Zh. Éksp. Teor. Fiz. **121**, 1051 (2002) [JETP **94**, 901 (2002)].
23. Yu. E. Danilova and V. P. Safonov, in *Proceedings of the 3rd Conference on Fractal in the Natural and Applied Sciences (IFIP), Marseille, 1995* (Chapman and Hall, London, 1995), pp. 102–112.
24. Yu. E. Danilova, V. A. Markel', and V. P. Safonov, Opt. Atmos. Okeana **6**, 1436 (1993).

Translated by V. Isaakyan